Orientational Dynamics and Dielectric Response of Nanopore Water

Jürgen Köfinger and Christoph Dellago

Faculty of Physics and Center for Computational Materials Science, University of Vienna, Boltzmanngasse 5, 1090 Vienna, Austria

(Received 6 April 2009; revised manuscript received 25 June 2009; published 17 August 2009)

We present numerical calculations, simulation results, and analytical considerations for the frequency-dependent dielectric constant of single-file water in narrow nanopores, described by a recently developed dipole lattice model. We find Debye relaxation over all length scales with relaxation times that strongly depend on pore length. This behavior is analyzed in terms of the dynamics of orientational defects leading to simple quantitative expressions for the static dielectric susceptibility and the relaxation time in the limits of short and long pores. Based on these formulas, we suggest how the predicted macroscopic order of nanopore water can be probed via dielectric spectroscopy and explain how the excitation energy, diffusion constant, and effective interaction of the defects that destroy the order can be extracted from such measurements.

DOI: 10.1103/PhysRevLett.103.080601 PACS numbers: 64.60.De, 05.50.+q, 52.25.Mq, 66.30.Lw

Inside narrow pores with subnanometer diameter, water forms single-file chains of hydrogen bonded molecules that are orientationally ordered over long distances [1,2]. The properties of nanopore water related to this one-dimensional (1D) structure are not only essential for living systems, where they determine water and ion transport across membranes, they also have implications for technical applications [3,4]. In particular, carbon nanotubes (CNTs) are promising building blocks for filtration, separation, and desalination devices as well as hydrogen fuel cells [5–8].

The orientational order arising from the particular interactions between water molecules strongly depends on length. Chains shorter than 0.1 mm are predominantly orientationally ordered with all water molecules pointing in the same direction [2]. Flips of the whole chain between the two equivalent states with opposite orientation are rare but do occur occasionally via the migration of hydrogen bonding defects. These defects consist of a molecule that either accepts two hydrogen bonds without donating any (D defect) or donates two hydrogen bonds without accepting any (L defect) and arise where chain segments with opposite orientation meet [8]. Chains longer than 0.1 mm are orientationally disordered and are composed of ordered domains separated by hydrogen bonding defects acting as domain walls. In such disordered chains, L and D defects alternate and flip the orientation of water molecules as they diffuse along the chain.

To date, these remarkable properties of nanopore water have been studied in detail using analytical theory and computer simulations but lack experimental verification. To remedy this situation, we investigate the response of nanopore water to a time-dependent homogeneous electric field in the direction of the tube axis and suggest how water chains inside pores can be probed experimentally by dielectric spectroscopy. The theoretical basis for our analysis is provided by a 1D dipole lattice model that accurately reproduces the free energetics of single-file water and permits extensive simulations despite the large length and time scales characteristic for the structure and dynamics of such chains [2,8,9]. This model provides the framework to determine, from dielectric spectroscopy experiments, the fundamental properties of nanopore water, namely, the excitation energy, the diffusion constant, and the effective interaction of hydrogen bonding defects.

In our model, water molecules are represented by dipoles with magnitude μ arranged on a 1D lattice with spacing a. The dipoles point either ''up'' or ''down'' the pore axis and are orthogonal to it in the case of defect molecules. It can be shown rigorously that the energy of the system, which is given by the sum of all dipole-dipole interactions, can be written as a sum of Coulomb-like interactions $q_i q_j a^{-1} \phi(|r_i - r_j| a^{-1})/(4\pi\varepsilon_0)$ of effective charges $q_i = \pm\mu/a$ carried by the defects and the chain ends, respectively [2,9]. Here $|r_i - r_j|$ is the distance between effective charges q_i and q_j, and ε_0 is the vacuum permittivity. The distance dependence of the interaction is given by $\phi(x) = [2\psi^{(1)}(x) + x\psi^{(2)}(x)] \approx 1/x + \mathcal{O}[x^{-3}]$, where $\psi^{(i)}(x)$ are polygamma functions. In this charge representation, which provides a physically appealing and transparent picture of the chain energetics, defects are formed by pairs of charges of equal magnitude which are negative for the L and positive for the D defect. For $a = 0.265$ nm and $\mu = 1.9975$ D, as obtained from molecular dynamics simulations, the effective defect charges have a magnitude of $2\mu/a \approx 0.31\ e$, and chain end points carry charges of half this magnitude [2].

We start our analysis by considering the linear response of the water wires to static electric fields as quantified by the static susceptibility χ, which is related to the equilibrium fluctuations of the total dipole moment M in the axis direction: $\chi = \beta\langle(\delta M)^2\rangle/(\varepsilon_0 N v)$. Here $\delta M = M - \langle M\rangle$ is the deviation of the total dipole from its canonical average, $\beta = 1/k_B T$ is the reciprocal temperature, v is

the volume per particle, and N is the number of molecules. Susceptibilities determined using Monte Carlo simulations [9] for two temperatures $T = 298$ K and $T = 387$ K are depicted in Fig. 1 as a function of chain length N. To compute χ from the dipole fluctuations, a volume per molecule of $v = 106$ nm^3 was used, corresponding to a membrane of uncorrelated water chains with an experimentally feasible pore density of 2.5×10^{11} cm^{-2} as recently realized in a CNT membrane with sub-2-nanometer pore diameters [10]. (Note, however, that pores of this size are still slightly to wide to support single-file water chains.) The χ vs N curves show two distinct regimes. While for short chains the susceptibilities grow linearly with chain length N, they saturate at large values in the long chain limit. For $T = 298$ K, the susceptibility $\chi \approx 8000$, which is about 100 times larger than the susceptibility of bulk water at ambient conditions ($\chi \approx 80$) even though the water density in the membrane is more than 3000 times smaller than that in the bulk.

The two different regimes of $\chi(N)$ are a consequence of the distinct nature of dipole fluctuations in short and long water chains. For small N, the chains are predominantly ordered with all dipoles pointing either up or down the tube axis such that the total dipole takes only the values $M = \pm N\mu$ [11]. Consequently, $\langle(\delta M)^2\rangle = N^2\mu^2$ leading to

$$\chi_{\text{short}}(N) = \frac{\beta\mu^2}{\varepsilon_0 v} N. \tag{1}$$

For large N, the order is destroyed by orientational defects as expected from the statistical mechanics of 1D systems, and the dipole fluctuations are determined by the defect statistics [2]. Since for ambient conditions the defect excitation energy $E_{\mathcal{D}}$ is large compared to the thermal energy $k_B T$, the defect density is low, leading to a large average defect distance of the order of $l \approx a \exp(\beta E_{\mathcal{D}})$. Therefore, the defect interactions are negligible, and the defects are uncorrelated to a very good approximation. In this limit,

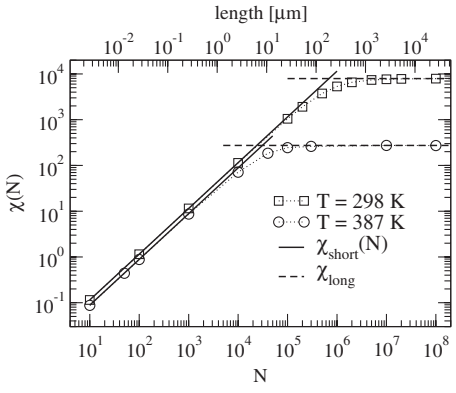

FIG. 1. The static dielectric susceptibility as a function of the tube length (top axis) and number of molecules (bottom axis). Symbols indicate simulation results for $T = 298$ K (squares) and $T = 387$ K (circles). Lines indicate approximations for short (solid) and long (dashed) pores.

the dipole model is isomorphic to the 1D Ising model with orientational defects corresponding to domain walls. This correspondence is established by choosing a coupling constant of $J = E_{\mathcal{D}}/2$ in the Ising case, as obtained by equating the domain wall energies in the two models. From the analytical solution of the 1D Ising model [12], one obtains $\langle(\delta M)^2\rangle = N^2\mu^2 e^{\beta E_{\mathcal{D}}}$ yielding the dielectric susceptibility for large N:

$$\chi_{\text{long}} = \frac{\beta\mu^2}{\varepsilon_0 v} e^{\beta E_{\mathcal{D}}}. \tag{2}$$

The predictions of Eqs. (1) and (2), shown in Fig. 1, reproduce the numerical results very well in the short and long chain limits, respectively. The chain length, at which the crossover between these two regimes occurs, can be estimated by equating Eqs. (1) and (2), yielding $N = \exp(\beta E_{\mathcal{D}}) \approx 7 \times 10^5$ for $T = 298$ K. At this system size, the chain contains a single defect on average.

Using Eqs. (1) and (2), one can extract the defect excitation energy $\beta E_{\mathcal{D}}$ and the magnitude μ of the dipole moment from measurements of the static susceptibility as a function of N. Further information can be obtained by analyzing the response of the chain to a time-dependent electric field as quantified by the frequency-dependent complex dielectric constant, related to the dipole autocorrelation function $\langle M(0)M(t)\rangle$ via the fluctuation-dissipation theorem [13].

As shown earlier [7,8], the dynamics of water chains is essentially determined by the diffusive migration of orientational defects under the influence of their mutual interactions. To model this kind of dynamics, we incorporate the motion of defects as a discrete time Markov process into our lattice model. The algorithm works as follows. In each step, one dipole is selected at random with uniform probability. The dipole is then subjected to a trial move, which is accepted or rejected depending on the energy change according to the Metropolis rule [14]. The possible trial moves are designed to mimic the natural, diffusive motion of defects and depend on the position and orientation of the selected dipole. If the dipole happens to be a defect, it is displaced by one lattice site to the left or right with equal probability.

Depending on the position of the defect, this translational move may result in its annihilation at the chain end or its recombination with a defect of opposite charge. For a dipole at a chain end, the trial move consists in the generation of a single defect, while for a dipole in the interior of an ordered domain, the generation of a defect pair is attempted. This pair consists of an L and a D defect separated by an intermediate dipole. After one sweep, consisting of N trial moves, time is advanced by the increment Δt. Since the generation probability for a defect pair away from other defects is known analytically, an event-driven version of this algorithm can be implemented, which leads to speedups of several orders of magnitude

and makes the simulations presented here possible [15]. Simulation time is related to real time by considering the diffusive motion of a single defect along the dipole chain. From molecular dynamics simulations it is known that orientational defects migrate with a diffusion constant of about $D = 0.04\ \mathrm{nm}^2/\mathrm{ps}$ [8] leading to a time increment of $\Delta t = a^2/2D \approx 0.88$ ps.

Using this algorithm, we have computed dipole autocorrelation functions $\langle M(0)M(t)\rangle$ for various system sizes and temperatures. In all size regimes, we observe Debye behavior for times longer than several hopping times Δt; i.e., the autocorrelation functions decay exponentially: $\langle M(0)M(t)\rangle = \langle M^2\rangle e^{-t/\tau}$. This is in contrast to the dielectric response of water clusters encapsulated in wider single-walled CNTs, which display Kohlrausch-William-Watts relaxation [16]. For Debye behavior, the complex dielectric constant is completely determined by $\langle M^2\rangle$ and τ [13]. Relaxation times τ of the dipole autocorrelation functions obtained as a function of N from fits to the simulation data are shown in Fig. 2 for two temperatures. Note that the frequencies corresponding to the observed relaxation times lie within the spectrum accessible in dielectric spectroscopy experiments. For both temperatures, the relaxation time grows monotonically with system size, and three distinct regimes can be identified. For short chains, the relaxation time grows sublinearly with N. Then, for intermediate chain lengths, the relaxation time increases linearly, before it converges to a constant value in the long chain limit. For these three regimes, which reflect different relaxation modes for the total dipole moment, simple expressions for $\tau(N)$ can be obtained as discussed in the following.

The dynamics of short chains consists of long permanences in the two perfectly ordered states with dipoles pointing up or down the tube axis, punctuated by rapid transitions between them occurring via defect migration. The resulting two-state behavior is the origin of exponential decay of the dipole autocorrelation function. In this size regime, the probability of finding more than one defect is negligible such that the total dipole moment of the chain is uniquely related to the defect position. Therefore, we can model the dipole dynamics as a nonlinear one-step hopping process (NOSHP) [17]. Here a defect located at site n hops to the neighboring sites $n-1$ and $n+1$ with transition rates r_n and g_n, respectively. These transitions rates are related to each other by the requirement of detailed balance $g_n/r_{n+1} = \exp(-\beta\Delta F_n)$, where $\Delta F_n = F_{n+1} - F_n$ and F_n is the free energy of the defect located at site $1 < n < N$. The free energy with respect to the fully ordered chain is given by $F_n = E_{\mathcal{D}} - \epsilon[\phi(n-1) + \phi(n) + \phi(N-n) + \phi(N-n+1) - 2\phi(N)] - k_BT\ln 2$, where $\epsilon = \mu^2/(4\pi\varepsilon_0 a^3)$ is the energy scale for the dipolar interactions. The term $k_BT\ln 2$ in the free energy accounts for the two reaction channels available for the chain flip—one for the diffusion of an L defect and one for that of a D defect. In the NOSHP the relaxation time is given by

$$\tau_{\mathrm{short}}(N) = \frac{1}{2}\sum_{\nu=1}^{N-1} g_\nu^{-1} e^{\beta F_\nu} \sum_{\mu=1}^{\nu} e^{-\beta F_\mu}. \tag{3}$$

Relaxation times determined from Eq. (3) for rates corresponding to Metropolis dynamics, $g_n = (2\Delta t)^{-1} \times \min\{1, \exp(-\beta\Delta F_n)\}$, are shown in Fig. 2 and agree well with the simulation results in the two-state regime. Solving Eq. (3) for rates corresponding to Glauber dynamics [18], $g_n = \Delta t^{-1}[1 + \exp(\beta\Delta F_n)]^{-1}$, yields essentially identical results indicating that the results do not depend on the details of the dynamics. Since Eq. (3) depends on the energy constant ϵ, it can be fitted to experimental results to determine the magnitude μ of the dipole moment.

A simpler expression for the relaxation time can be obtained by approximating the free energy landscape felt by the migrating defect by a rectangular profile of width $N-2$ and height $F_{N/2}$. With the barrier height given by $F_{N/2} \approx E_{\mathcal{D}} - 6\epsilon/N - k_BT\ln 2$, we solve Eq. (3) analytically obtaining

$$\tau_{\mathrm{short}}(N) \approx e^{\beta(E_{\mathcal{D}} - 6\epsilon/N)} \frac{Na^2}{4D}, \tag{4}$$

which reproduces simulation results for small chain lengths qualitatively (see Fig. 2). The term proportional to $1/N$ in the exponential of Eq. (4), which causes the curvature of the τ vs N curves for short chains, is a reflection of the Coulomb-like attraction of the defect at the chain center with the end points of the chain, thus providing a way to verify this interaction experimentally. For increasing chain length, this attraction decreases and can be neglected for sizes $N \gtrsim 1000$. Then the relaxation time increases linearly with chain length with a slope that depends on the defect energy.

The linear behavior of $\tau(N)$, a manifestation of the two-state behavior with constant barrier height but growing barrier width, persists until a size is reached where more

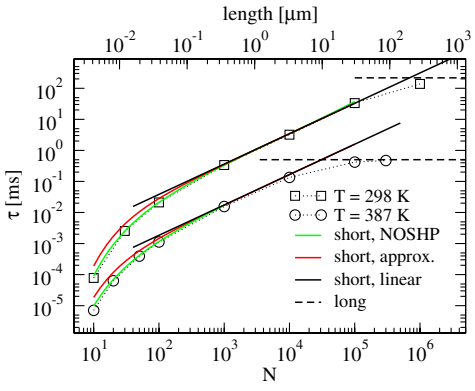

FIG. 2 (color online). The relaxation time as a function of the tube length (top axis) and number of molecules (bottom axis). Simulation results are shown for $T = 298$ K (squares) and $T = 387$ K (circles). Also shown are relaxation times calculated in the short and long chain limits.

than one defect is present in the chain on average. The crossover to this regime occurs at $N \approx \exp(\beta E_{\mathcal{D}})$. For large tube lengths and uncorrelated defects, our model is dynamically isomorphic to the kinetic Ising model in one dimension. In this case, the autocorrelation function of the total magnetization of the Ising model decays exponentially with a relaxation time of $\tau = \Delta t(1-\gamma)^{-1}$, where $\gamma = \tanh(\beta E_{\mathcal{D}})$ [18]. For large defect energies, Glauber's expression simplifies to

$$\tau_{\text{long}} \approx e^{2\beta E_{\mathcal{D}}} \frac{a^2}{4D}. \tag{5}$$

Thus, in the large system limit the relaxation time converges to a constant value in good agreement with the relaxation times found in our dynamical Monte Carlo simulations. By combining Eqs. (4) and (5), one can use the size dependence of the relaxation time in the linear and constant regime to determine the defect energy $E_{\mathcal{D}} = -k_B T \ln(s/\tau_{\text{long}})$, where s is the slope of the relaxation time as a function of N in the linear regime. The diffusion constant of the defects is then given by $D = a^2 \tau_{\text{long}}/(4s^2)$.

Note that in the above analysis we have assumed that D and L defects have the same defect energy $E_{\mathcal{D}}$ and migrate with the same diffusion constant D. Simulations indicate that this assumption holds to a considerable degree, but nevertheless differences exist [8,19–21]. Thus, the procedure suggested here yields average values of $E_{\mathcal{D}}$ and D lying between the corresponding true values for the D and L defects. However, large differences in the defect energy lead to deviations from the predicted behavior in the two-state regime that could be detected in experiments [15].

In summary, we have clarified how dielectric spectroscopy can serve to probe the properties of water confined to the interior of narrow pores. Our computer simulations demonstrate that the dielectric response of such nanopore water follows Debye behavior. We find that the time evolution of the total dipole moment of a 1D water chain is determined by the diffusive dynamics of essentially uncorrelated defects and derive simple and accurate formulas for the susceptibility and relaxation time as a function of chain length. These expressions, verified in extensive simulations, permit one to extract fundamental molecular information such as the energy, diffusion constant, and interactions of defects from dielectric relaxation spectra.

The experimental studies suggested in this Letter may be carried out using membranes of nonmetallic CNTs with subnanometer diameter. Compared to current CNT membranes [5], meeting this experimental challenge will require further reduction in pore diameter and selection of appropriate chirality. Other possibilities to observe single-file dipole chains include water or other dipolar hydrogen bonding molecules confined in boron-nitride tubes [20,22] or silanized channels across silicon wafers [23] as well as confined colloidal particles with permanent magnetic or electric dipole moments [24–26]. Because of the strong length dependence of the dielectric response of 1D water chains, with the static dielectric susceptibility and the relaxation time spanning orders of magnitude, water-filled CNTs may serve as capacitors, e.g., in sensing devices [27,28].

We thank G. Hummer, G. Menzl, and W. Schranz for useful discussions. We acknowledge support from the Austrian Science Fund (FWF) under Grants No. P20942-N16 and No. W004 and from the University of Vienna through the Focus Research Area *Materials Science*.

[1] G. Hummer, J. C. Rasaiah, and J. P. Noworyta, Nature (London) **414**, 188 (2001).
[2] J. Köfinger, G. Hummer, and C. Dellago, Proc. Natl. Acad. Sci. U.S.A. **105**, 13 218 (2008).
[3] J. C. Rasaiah, S. Garde, and G. Hummer, Annu. Rev. Phys. Chem. **59**, 713 (2008).
[4] B. Hille, *Ion Channels of Excitable Membranes* (Sinauer Associates, Inc., Sunderland, 2001), 3rd ed.
[5] J. K. Holt *et al.*, Science **312**, 1034 (2006).
[6] A. Kalra, S. Garde, and G. Hummer, Proc. Natl. Acad. Sci. U.S.A. **100**, 10 175 (2003).
[7] C. Dellago and G. Hummer, Phys. Rev. Lett. **97**, 245901 (2006).
[8] C. Dellago, M. M. Naor, and G. Hummer, Phys. Rev. Lett. **90**, 105902 (2003).
[9] J. Köfinger, G. Hummer, and C. Dellago, J. Chem. Phys. **130**, 154110 (2009).
[10] F. Fornasiero *et al.*, Proc. Natl. Acad. Sci. U.S.A. **105**, 17 250 (2008).
[11] S. Vaitheeswaran, J. C. Rasaiah, and G. Hummer, J. Chem. Phys. **121**, 7955 (2004).
[12] R. J. Baxter, *Exactly Solved Models in Statistical Mechanics* (Dover, New York, 2007).
[13] D. A. McQuarrie, *Statistical Mechanics* (University Science Books, New York, 2000), 2nd ed.
[14] M. Metropolis *et al.*, J. Chem. Phys. **21**, 1087 (1953).
[15] J. Köfinger and C. Dellago (to be published).
[16] Z. Dendzik, M. Kośmider, and M. Sokół, J. Non-Cryst. Solids **354**, 4300 (2008).
[17] N. G. van Kampen, *Stochastic Processes in Physics and Chemistry* (Elsevier, Amsterdam, 1992).
[18] R. J. Glauber, J. Math. Phys. (N.Y.) **4**, 294 (1963).
[19] U. Zimmerli *et al.*, Nano Lett. **5**, 1017 (2005).
[20] C. Y. Won and N. R. Aluru, J. Phys. Chem. C **112**, 1812 (2008).
[21] R. B. Best and G. Hummer, Proc. Natl. Acad. Sci. U.S.A. **102**, 6732 (2005).
[22] C. Y. Won and N. R. Aluru, J. Am. Chem. Soc. **129**, 2748 (2007).
[23] D. Xu *et al.*, New J. Chem. **27**, 300 (2003).
[24] K. Butter *et al.*, Nature Mater. **2**, 88 (2003).
[25] B. H. Erne *et al.*, J. Magn. Magn. Mater. **311**, 145 (2007).
[26] V. F. Puntes, K. M. Krishnan, and P. Alivisatos, Appl. Phys. Lett. **78**, 2187 (2001).
[27] S. K. Saha and D. Chakravorty, Appl. Phys. Lett. **89**, 043117 (2006).
[28] D. V. Matyushov, J. Chem. Phys. **127**, 054702 (2007).